

## Highlights

**This is a specimen  $a_b$  title**

C. Tasich,Han Theh Thanh,CV Rajagopal,Rishi T.

- Research highlights item 1
- Research highlights item 2
- Research highlights item 3

# This is a specimen $a_b$ title<sup>\*,\*\*</sup>

C. Tasich<sup>a,c,\*,1</sup> (Researcher), Han Theh Thanh<sup>b,d</sup>, CV Rajagopal Jr<sup>b,c,2</sup> (Co-ordinator) and Rishi T.<sup>a,c,\*,1,3</sup>

<sup>a</sup>Elsevier B.V., Radarweg 29, 1043 NX Amsterdam, The Netherlands

<sup>b</sup>Sayahna Foundation, Jagathy, Trivandrum 695014, India

<sup>c</sup>STM Document Engineering Pvt Ltd., Mepukada, Malayinkil, Trivandrum 695571, India

## ARTICLE INFO

### Keywords:

quadrupole exciton

polariton

WGM

BEC

## ABSTRACT

This template helps you to create a properly formatted L<sup>A</sup>T<sub>E</sub>X manuscript.

`\beginabstract... \endabstract` and `\begin{keyword} ... \end{keyword}` which contain the abstract and keywords respectively. Each keyword shall be separated by a `\sep` command.

## 1. Introduction

## 2. Methods

We modeled tidal platform elevation ( $\zeta$ ) using a zero-dimensional mass balance model using the basic formulation provided by Krone Krone (1987) and further refined by Allen Allen (1990), French French (1993), and Temmerman et al. Temmerman, Govers, Meire and Wartel (2003); Temmerman, Govers, Wartel and Meire (2004). The rate of tidal platform elevation change is described as

$$\frac{d\eta}{dt} = \frac{dS_M}{dt} + \frac{dS_O}{dt} + \frac{dP}{dt} + \frac{dM}{dt}, \quad (1)$$

where  $S_M$  is mineral sedimentation,  $S_O$  is organic matter sedimentation,  $P$  is compaction, and  $M$  is tectonic subsidence. Each term of equation 1 can be further expanded.

We approximate  $S_M$  as

$$S_M(t) = \int \frac{w_s C(t)}{\rho_b} dt, \quad (2)$$

where  $w_s$  is the characteristic settling velocity of a given grain size,  $C(t)$  is the depth-averaged and time-varying sediment concentration in the water column, and  $\rho_b$  is the dry bulk density of the sediment. We assume there is no resuspension of mineral sediment which is consistent with Krone's Krone (1987) initial formulation.

$w_s$  is calculated for a given grain size by using Stokes' law to determine the terminal velocity of a sphere falling through a fluid given by

$$w_s = \frac{2}{9} \frac{\rho_p - \rho_f}{\mu} g R^2 \quad (3)$$

\* This document is the results of the research project funded by the National Science Foundation.


\*\* The second title footnote which is a longer text matter to fill through the whole text width and overflow into another line in the footnotes area of the first page.

This note has no numbers. In this work we demonstrate  $a_b$  the formation Y\_1 of a new type of polariton on the interface between a cuprous oxide slab and a polystyrene micro-sphere placed on the slab.

\*Corresponding author

\*\*Principal corresponding author

 [chris.tasich@vanderbilt.edu](mailto:chris.tasich@vanderbilt.edu) (C. Tasich); [cvr3@sayahna.org](mailto:cvr3@sayahna.org) (C. Rajagopal); [rishi@stmdocs.in](mailto:rishi@stmdocs.in) (R. T.)

 [www.cvr.cc](http://www.cvr.cc), [cvr@sayahna.org](http://cvr@sayahna.org) (C. Tasich); [www.sayahna.org](http://www.sayahna.org) (C. Rajagopal); [www.stmdocs.in](http://www.stmdocs.in) (R. T.)

ORCID(s): 0000-0001-7511-2910 (C. Tasich)

<sup>1</sup>This is the first author footnote. but is common to third author as well.

<sup>2</sup>Another author footnote, this is a very long footnote and it should be a really long footnote. But this footnote is not yet sufficiently long enough to make two lines of footnote text.

where  $\rho_p$  is the mass density of the particle or grain,  $\rho_f$  is the mass density of the fluid,  $\mu$  is the dynamic viscosity of the fluid,  $g$  is the acceleration due to gravity, and  $R$  is the radius of the grain. This is approximation for  $w_s$  is consistent with previous similar studies Allen (1990); Temmerman et al. (2003, 2004). We assume basic properties of water for  $\rho_f$  ( $1000 \text{ kg m}^{-3}$ ) and  $\mu$  ( $1 \times 10^{-3} \text{ kg m}^{-1} \text{ s}^{-1}$ ) for simplicity. Salinity does vary seasonally which will change these values, but had little affect on the model output.

We capture the temporal variation of  $C(t)$  through the mass balance given as

$$\frac{d[h(t) - \zeta(t)]C(t)}{dt} = -w_s C(t) + C_{in} \frac{dh}{dt}, \quad (4)$$

where  $h$  is the height of the water column and  $C_{in}$  is the incoming suspended sediment concentration of the adjacent water column. We consider  $\zeta$  to be a function of time and update it at every timestep which differs from previous studies Krone (1987); Allen (1990); French (1993); Temmerman et al. (2003, 2004); French (2006) which only update  $\zeta$  after every tidal cycle. The physical interpretation of equation 4 is that the first term is the mass flux above an area on the tidal platform, the second term is the mass flux extracted from the water column, and the third term is the mass flux from the adjacent water column. Further derivation of equation 4 results in

$$\frac{dC}{dt}[h(t) - \zeta(t)] = -w_s C(t) + [C_{in} - C(t)] \frac{dh}{dt} + C(t) \frac{d\zeta}{dt} \quad (5)$$

From equation 5, we can approximate the solution for concentration numerically.

## Model inputs

We obtained model inputs from field measurements. We observed tidal height, grain size, suspended sediment concentration (SSC), and dry bulk density around Polder 32 over multiple field seasons from 2011 to 2016 Auerbach, Jr, Mondal, Wilson, Ahmed, Roy, Steckler, Small, Gilligan and Ackerly (2015); Hale, Bain, Goodbred Jr. and Best (2019a); Hale, Wilson and Bomer (2019b).

For  $h$ , we extracted one year of contiguous tidal data from from a pressure sensor deployed within the tidal channel near Polder 32. We used the oce package in R (3.6.3) to create an idealized tidal curve from our data ?. The tidal curve was then shifted down so that mean higher high water would be 0.3 m above the Sundarban platform and 1.8 m above the polder surface ( $\zeta$ ). We replicated this tidal curve for each subsequent year for the length of the model run. Field observations confirm these benchmark elevation Auerbach et al. (2015); Hale et al. (2019b); Bomer, Wilson, Hale, Hossain and Rahman (2020). In order to simulate sea level rise, the subsequent year tidal curves were increased at a linear rate of  $2 \text{ mm yr}^{-1}$  which is consistent with field observations.

For  $C_{in}$ , we use observed values of SSC from Hale et al. Hale et al. (2019a) that are characteristic of the tidal channels in the region. Similar to Temmerman et al. Temmerman et al. (2003, 2004), we scaled the observed tidal channel SSC by a factor as the flood waters are expected to have a lower SSC than the tidal channel due to lower flow velocities. For our preliminary study, we use a k-factor of 0.7. In future model iterations, we will better explore this relationship and determine an appropriate k-factor.

For  $\rho$ , we used values derived from conversations with Steven Goodbred and Carol Wilson.

## 3. Results

## 4. Discussion

## 5. Conclusions

## 6. Bibliography

## CRediT authorship contribution statement

**C. Tasich:** Conceptualization of this study, Methodology, Software. **CV Rajagopal:** Data curation, Writing - Original draft preparation.

## References

- Allen, J.R.L., 1990. Salt-marsh growth and stratification: A numerical model with special reference to the Severn Estuary, southwest Britain. *Marine Geology* 95, 77–96. doi:10/dpcnnc.
- Auerbach, L.W., Jr, S.L.G., Mondal, D.R., Wilson, C.A., Ahmed, K.R., Roy, K., Steckler, M.S., Small, C., Gilligan, J.M., Ackerly, B.A., 2015. Flood risk of natural and embanked landscapes on the Ganges–Brahmaputra tidal delta plain. *Nature Climate Change* 5, 153–157. doi:10/gc3fxh.
- Bomer, E.J., Wilson, C.A., Hale, R.P., Hossain, A.N.M., Rahman, F.M.A., 2020. Surface elevation and sedimentation dynamics in the Ganges–Brahmaputra tidal delta plain, Bangladesh: Evidence for mangrove adaptation to human-induced tidal amplification. *CATENA* 187, 104312. doi:10/ggszhr.
- French, J., 2006. Tidal marsh sedimentation and resilience to environmental change: Exploratory modelling of tidal, sea-level and sediment supply forcing in predominantly allochthonous systems. *Marine Geology* 235, 119–136. doi:10/ccdv2v.
- French, J.R., 1993. Numerical simulation of vertical marsh growth and adjustment to accelerated sea-level rise, North Norfolk, U.K. *Earth Surface Processes and Landforms* 18, 63–81. doi:10/drw2f8.
- Hale, R., Bain, R., Goodbred Jr., S., Best, J., 2019a. Observations and scaling of tidal mass transport across the lower Ganges–Brahmaputra delta plain: Implications for delta management and sustainability. *Earth Surface Dynamics* 7, 231–245. doi:10/gf2cdq.
- Hale, R.P., Wilson, C.A., Bomer, E.J., 2019b. Seasonal Variability of Forces Controlling Sedimentation in the Sundarbans National Forest, Bangladesh. *Frontiers in Earth Science* 7, 211. doi:10/ggjhb2.
- Krone, R., 1987. A Method for Simulating Marsh Elevations, in: *Coastal Sediments*, American Society of Civil Engineers, New Orleans, Louisiana. pp. 316–323.
- Temmerman, S., Govers, G., Meire, P., Wartel, S., 2003. Modelling long-term tidal marsh growth under changing tidal conditions and suspended sediment concentrations, Scheldt estuary, Belgium. *Marine Geology* 193, 151–169. doi:10/dqg2zs.
- Temmerman, S., Govers, G., Wartel, S., Meire, P., 2004. Modelling estuarine variations in tidal marsh sedimentation: Response to changing sea level and suspended sediment concentrations. *Marine Geology* 212, 1–19. doi:10/dsjcj6.